FOREX Publication
Open Access | Rapid and quality publishing

International Journal of
Electrical and Electronics Research (IJEER)
Research Article | Volume 12, Issue 3 | Pages 951-956 | e-ISSN: 2347-470X

Improvement of Solar Farm Performance based on Photovoltaic Modules Selection

Suy Kimsong[1*], Horchhong Cheng[2], Chivon Choeung[3], Sophea Nam[4] and Darith Leng[5]

[1]Graduate School, National Polytechnic Institute of Cambodia, Phnom Penh, Cambodia; suykimsong@npic.edu.kh
[2,3,4]Faculty of Electricity, National Polytechnic Institute of Cambodia, Phnom Penh, Cambodia; horchhong@gmail.com[2], choeungchivon@npic.edu.kh[3], namsophea@npic.edu.kh[4]
[5]Power System Analysis Division, Electricity of Cambodia, Phnom Penh, Cambodia; darith.leng@gmail.com

***Correspondence:** Suy Kimsong; *suykimsong@npic.edu.kh*

ABSTRACT- The emissions of greenhouse gases from conventional power plants are currently a significant cause for worry. In China, about 75% of total domestic energy is dependent on coal-fire power, which emits 50% of total SO2 and has a significant impact on the human respiratory system. Therefore, solar power plants are a viable option that can mitigate this problem. Furthermore, the efficiency of solar modules exhibits a progressive upward trend, while their price per watt experiences a corresponding decline, making it a promising source for future energy. This article examines the performance and effectiveness of several photovoltaic (PV) modules in designing solar plants on a certain land area measuring 10000 m2 (100 m * 100 m). The PV plant performance was evaluated by comparing occupation ratio (OR), PV power capacity, net energy production, performance ratio (PR) via PVsyst software, and lastly financial analysis. Consequently, the PV module (PV7), characterized by its high efficiency, low temperature coefficients, and affordable price, result in a significant OR (73.81%), increased installed PV power capacity (1568kW), enhanced net energy output (2269029 kWh/year), improved yearly PR (83.4%), and lastly, the shortest payback period (around two years). Instead of optimizing shadow length in existing research, this paper aims to improve the performance of large-scale solar farm based on PV module selection which results in less computation and structure installation efforts.

Keywords: Photovoltaic module; Performance ratio; Temperature coefficient; Solar; PV power.

ARTICLE INFORMATION

Author(s): Suy Kimsong, Horchhong Cheng, Chivon Choeung, Sophea Nam and Darith Leng;

Received: 08/06/2024; **Accepted**: 30/07/2024; **Published**: 20/08/2024;
e-ISSN: 2347-470X;
Paper Id: IJEER 0806-08;
Citation: 10.37391/ijeer.120328
Webpage-link:
https://ijeer.forexjournal.co.in/archive/volume-12/ijeer-120328.html

Publisher's Note: FOREX Publication stays neutral with regard to Jurisdictional claims in Published maps and institutional affiliations.

1. INTRODUCTION

The Department of Economic and Social Affairs of the United Nations estimates that the global population will increase by over 10 billion by 2059 [1]. This indicates the need for an abundance of energy in the future. However, nearly all global energy sources are non-renewable, contributing to global warming through greenhouse gas (GHG) emissions, a concern that is gravely endangering human life. In China, about 75% of total domestic energy is dependent on coal-fire power, which emits 50% of total SO_2 and has a significant impact on the human respiratory system [2]. Due to environmental concern and energy security for sustaining human life, alternative energy sources (renewable energy sources) play an important role in meeting the needs of global energy demand. Around the world, solar energy is clean and abundant, making it a promising source for future energy. Additionally, In case of Cambodia, the government has set a policy to phase out all coal power plants by 2050 and encourage the use of PV power instead. [3] reports that between 2017 and 2022, the installed solar farm capacity reached 335 MW, which then fed into the Cambodian national grid. And, the average solar radiation in Cambodia is approximately 5 kWh/m^2, which is higher than some nations such as Thailand, China, and Germany [4]. The development of PV energy application was extended all around the world, more than 145,000 home PV systems and more than 1 GW of PV deployed by US utilities were installed in the US in the first half of 2013 [5]. However, installations have not just occurred in the US. Further ambitious renewable energy programs have also been implemented in Spain, China, Japan, Germany, and numerous other nations [6]. Crystalline silicon (c-Si) panels, which are among the earliest generation of PV panels, account for 95% of all solar PV panels made globally [7]. Because silicon, the main component of c-Si, has economies of scale over other materials, it is more cost-effective and efficient than other materials. The efficiency and power output of solar panels have grown dramatically in the last few decades. PV panels with mono crystalline and multi crystalline structures have average module efficiencies of 14.7% and 13.2%, respectively, in 2006. Since then, there has been a sharp increase in average module efficiency, reaching 17% and 18%, respectively. This rising trend is expected to continue until 2030 [7].

Taking advantage of this, many researchers are interested and have done much research on solar cell fabrication technology, PV system stability, energy storage system technology, PV module degradation, and mounting structure to improve and

FOREX Publication
Open Access | Rapid and quality publishing
International Journal of Electrical and Electronics Research (IJEER)
Research Article | Volume 12, Issue 3 | Pages 951-956 | e-ISSN: 2347-470X

stabilize solar energy systems. In [8], a planar perovskite solar cell could achieve 15.49% efficiency via a low-temperature process with brookite TiO_2. And [9] the author used the combination between a poly-Si cell and an a-Si cell at low temperature; consequently, the cell efficiency could reach 12% and the temperature coefficient was 0.268%. Another thing is that the control algorithm is also the main key to maintaining PV system stability. In [10], researchers used modified droop control and a virtual synchronous generator (VSG) algorithm to observe how well a standalone PV system could maintain its transient response. In [11], the author used a virtual synchronous generator (VSG) along with hybrid energy storage to keep the system frequency stable during changes in PV power. This made the overshoot frequency deviation smaller, from 50.18 Hz to 50.03 Hz. Currently, short-term installation and low maintenance costs [12] have synchronized large-scale PV plants to the grid. However, economic growth has led to an increase in land costs [13], posing a major obstacle to PV installation in large open areas. Therefore, to address this issue, the optimization of PV plant performance is developed. Rooftop PV systems are an option to save space. Xiagyang et al. [14] designed a 43.2 kW grid-connected rooftop PV system to optimize power utilization and reduce grid power sales. A dual-axis PV system that could obtain energy 24.6% greater than a fixed PV system is designed in [15]. An optimal voltage regulation is proposed in [16] for PV-connected inverter. Similarly, method [17] presented a simulation of PV system operation in both grid-connected and standalone modes. Additionally, [18] have studied the estimation of PV plant performance with the optimization of tile angle, and at 15° tile angle, the plant performance ratio reached 82%. According to [19], the 0.3kW scale of a mirror integrated solar PV system (MISPVS) provides a net energy of 30.30% more than that of a traditional PV system (TSPVS). Method [20] demonstrated how a parabolic trough and Fresnel mirror solar concentrator could enhance the power of PV panels by 26.81% and 17.89%, respectively. Pravesh et al. [21] conducted a study on improving PV panels using back water-cooling tubes, resulting in an efficiency increase from 0.5 to 1%. [22] modeled and simulated a 1 MW PV power plant in Iraq, while [23] described a suitable site selection for a 10 MW PV capacity installation in Saudi Arabia. [24] conducted a shading analysis to minimize land area, resulting in a 25% increase in PV plant capacity for the given land area. But none of the previously mentioned research was considered when choosing between various PV module options in terms of performance analysis. In addition, [25] reported that the best PV panel was chosen for the PV system design based on a comparison of electrical, mechanical, financial, environmental, and customer characteristics.

However, the estimation of OR, installed PV capacity, energy production, PR, and payback period of the chosen PV modules for large-scale PV plant design on a given land area has not yet been studied.

The PV plant used in this study was developed using a typical mounting structure, with the assumption that the collector plane's tile angle would equal the latitude angle. On the other hand, the M-shaped mounting structure and shadow length analysis have not yet been examined in this paper.

This work aims to improve the performance of large-scale solar farms based on eight PV modules selection installed on given land area 10000 m^2 by comparing OR, installed PV power capacity, net energy production, PR, and includes a financial analysis via PVsyst software, which results in less calculation and structural installation efforts, as compared to optimizing shadow length as is the case in previous research.

2. MATERIALS AND METHODS

This study configures eight selected PV modules with a selected grid-tied inverter on a 10000 m^2 (100m*100m) land area, with the site located at latitude 11.20° and longitude 104.59°. The performance of eight selected PV modules is investigated by comparing the OR, installed PV power capacity, net energy production, and PR. The details of the system design are described below:

2.1. Choosing Photovoltaic Modules

PV modules are crucial components for incorporation into solar farms. There is a wide variety of PV modules available on the market, varying in types, sizes, costs, and effectiveness. Moreover, the price and efficiency of PV modules are the primary elements that might enhance the performance of a solar farm. Hence, it is imperative to select PV modules appropriately. For this investigation, a total of eight PV modules were chosen, and their technical information, such as maximum power (P_m), maximum voltage (V_m), maximum current (I_m), open circuit voltage (V_{OC}), short circuit current (I_m), temperature coefficient of P_m, and dimension, is presented in *table 1*.

2.2. Choosing a Grid-Tied Inverter

The solar energy is transmitted to the electrical grid by an inverter. The research involved selecting a 22kW grid-tied inverter to be paired with all PV modules listed in *table 1*. The specific features of the inverter can be found in *table 2*.

Table 1. The specific attributes of the chosen eight photovoltaic modules

PVModule Sample	P_m (W)	V_m(V)	I_m(A)	V_{OC} (V)	I_{SC} (A)	Eff (%)	Tem.Coefof Pm (%/°C)	Dimension
PV1	170	19.15	8.88	23.31	9.42	17.14	-0.4	(1480×670) mm^2
PV2	290	32.48	8.93	39.14	9.47	17.12	-0.4	(1650×992) mm^2
PV3	285	31.8	8.97	39	9.48	17.52	-0.39	(1640×992) mm^2
PV4	350	38.1	9.19	46.7	9.68	18.04	-0.39	(1956×992) mm^2
PV5	335	34.02	9.85	41.49	10.49	19.9	-0.37	(1690×996) mm^2
PV6	450	41.4	10.87	50	11.54	20.7	-0.35	(2094×1038) mm^2
PV7	660	37.8	17.46	45.9	18.43	21.27	-0.34	(2383×1302) mm^2
PV8	550	42.1	13.06	50.1	13.9	21.3	-0.35	(2278×1134) mm^2

FOREX Publication
Open Access | Rapid and quality publishing
International Journal of Electrical and Electronics Research (IJEER)
Research Article | Volume 12, Issue 3 | Pages 951-956 | e-ISSN: 2347-470X

Table 2. Specification of a Grid-Tied Inverter

DC side/input parameters			
Max. DC power (kW)	**The MPPT voltage range (V)**	**Max. input current/MPPT (A)**	**Number of MPPT trackers**
33	413-1100	27	2
AC side/output parameters			
AC Power (kW)	**Voltage (V)**	**Max. Current (A)**	**Efficiency (%)**
22	400	35.5	98

2.3. Setup of Photovoltaic Modules and an Inverter

2.3.1. Voltage Specification Matching

Equations (1) and (2) determine the voltage of the PV module for temperatures above and below 25 °C, respectively [26]. When the ambient temperature is below 25 °C, the cell temperature is assumed to be the same as the surrounding temperature. For ambient temperatures exceeding 25 °C, the cell temperature can be determined by using *equation (3).*

$$V_{m\,(at\,X\,^oC)} = V_m - \left[\gamma_v \times \left(T_{X\,^oC} - T_{STC}\right)\right] \quad (1)$$

$$V_{OC\,(at\,X\,^oC)} = V_{OC} + \left[\gamma_v \times \left(T_{X\,^oC} - T_{STC}\right)\right] \quad (2)$$

$$T_{X\,^oC} = T_a + 25^oC \quad (3)$$

Where $V_{m\,(atX\,^oC)}$ and $V_{OC\,(atX\,^oC)}$ are the voltage of PV module at ambient temperature higher and lower 25 °C respectively, γ_v is the temperature coefficient, $T_{X\,^oC}$ is the cell temperature, T_{STC} is the temperature at the standard test condition (STC), and T_a is the ambient temperature. *Equations (4) and (5)* can be used to calculate the minimum and maximum number of PV modules that can be connected in series per string, once the voltages of the PV modules are determined [27].

$$Min\,No.of\ module\,/\,string = \frac{V_{mppt(inv_{\min})}}{V_{m(atX\,^oC)}} \quad (4)$$

$$Max\,No.of\ module\,/\,string = \frac{V_{inv(\max)}}{V_{OC(at\,X\,^oC)}} \quad (5)$$

Where $MinNo.ofmodule/string$ is minimum number of PV modules per string, $V_{mppt(inv_{min}}$ is minimum mppt voltage of inverter, $MaxNo.ofmodule/string$ is maximum number of PV modules per string, and $V_{inv(max)}$ is maximum input voltage of inverter.

2.3.2. Current Specifications Matching

It is important to ensure that the current of the PV string does not surpass the current of the inverter, based on the information provided in Table 1 and 2. The number of photovoltaic (PV) strings per inverter can be determined by dividing the total input current of the inverter by the total current per PV string.

2.3.3. Matching Power of Photovoltaic Modules to the Power Rating of Inverter

Generally, the inverter achieves its highest efficiency when the power of the PV array is close to the power rating of the inverter. Therefore, the total power of PV modules per inverter can be determined by multiplying the total number of PV strings by the rated power of the PV modules connected in series per string.

2.4. Row Spacing Computation

Optimizing the land area in solar farm design is crucial for increasing the installed PV power capacity, and reducing the row spacing length can enhance land utilization for PV installation. However, the reduction in row spacing length must ensure that the PV strings escape from the shadow, as illustrated in *figure 1*, and the shadow length and row spacing can be calculated by *equations (6)* through (8) [19].

$$d_i = H/\tan(\alpha_{(min)}) \quad (6)$$

Where d_i is shadow length, $\alpha_{(min)}$ is altitude, and H is the height of the PV module, the height of the PV module can be calculated by *equation (7).*

$$H = l \times \sin\beta \quad (7)$$

Where l is the PV module length. And the row spacing can be calculated by *equation (8).*

$$d_{i(min)} = d_i \times \cos(180^o - A_{Zi}) \quad (8)$$

Where $d_{i(min)}$ is row spacing, and A_{Zi} is the azimuth angle. Additionally, according to *figure 2*, the lowest altitude occurs on December 22nd. Therefore, this date is used to define the azimuth (116.22°) and altitude (9.08°).

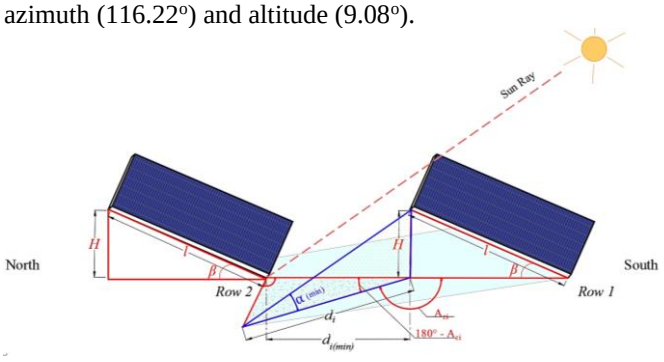

Figure 1. Side view of the PV string with shadow length

FOREX Publication
Open Access | Rapid and quality publishing
International Journal of Electrical and Electronics Research (IJEER)
Research Article | Volume 12, Issue 3 | Pages 951-956 | e-ISSN: 2347-470X

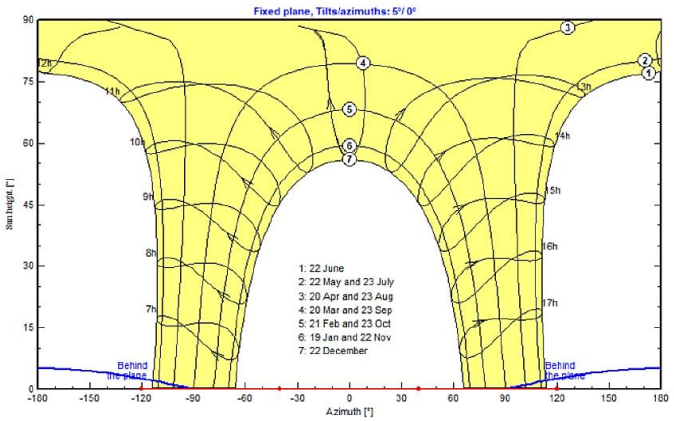

Figure 2. Sun path throughout the year

2.5. Performance Evaluation

Occupation ratio (OR) is defined by active PV modules area (S_{PV}) on given land area (S) as represent in *equation (9)* [19].

$$OR = \frac{S_{PV}}{S} \quad (9)$$

The total daily (E_D) and monthly (E_M) energy production of PV plant are depicted in *equation (10) and (11)* respectively [25].

$$E_D = \sum_{t=1}^{t=24} E_t \quad (10)$$

$$E_M = \sum_{D=1}^{n} E_D \quad (11)$$

Where t is the hour of the day and N is the day number of the months.

The Performance Ratio (PR), a ratio between net energy production (E_{grid}) and theoretical energy production (E_{PV}) of PV plants as defined in *equation (12)*[24].

$$PR = \frac{E_{grid}}{E_{PV}} \quad (12)$$

3. RESULTS AND DISCUSSIONS

PVsyst software is used in this study to evaluate the performance of eight selected PV modules. The system performance analysis is based on a comparison of OR, installed PV power capacity, net energy production, and, finally, PR. However, the financial analysis only considers the cost of PV modules, grid tie-inverters, land, and lastly selling energy.

3.1. Potential of Solar Radiation

Solar radiation is a key indicator of solar energy sources' potential. According to simulation result of PVsyst software, in *figure 3* shows the monthly solar radiation on the collector plane (at tilt angle 10°) throughout the year at the side location study, and the yearly average solar radiation is approximately 4.755 kWh/m^2/day, which is a potential value for photovoltaic system applications for site location.

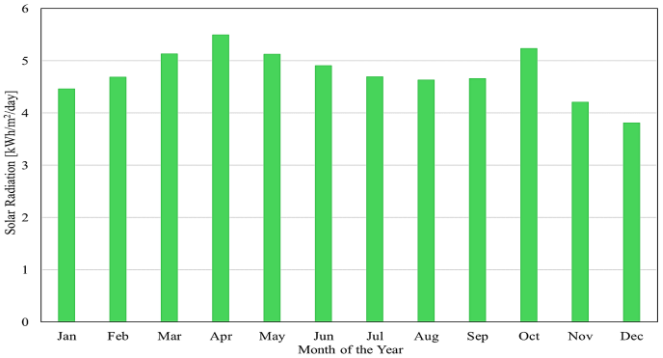

Figure 3. Solar radiation on the collector plane at tile angle 10°

3.2. Occupation Ratio and Installed PV Power Capacity

The occupation ratio (OR) is a ratio between the active area of modules on a given land area (10000 m^2). According to the technical data in *table 1*, PV7 has the highest efficiency (21.27%), leading to the highest value of OR (73.81%), whereas for the other seven PV modules, the value of OR is below 66%, as depicted in *figure 4(a)*. As a result, the PV7 selection has the greatest potential to increase the effectiveness of given land area utilization.

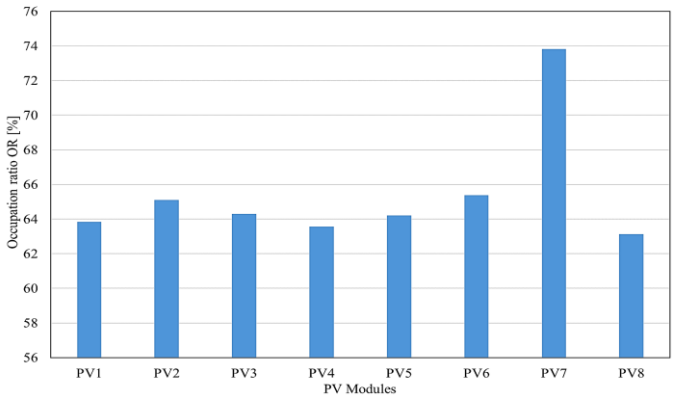

(a)

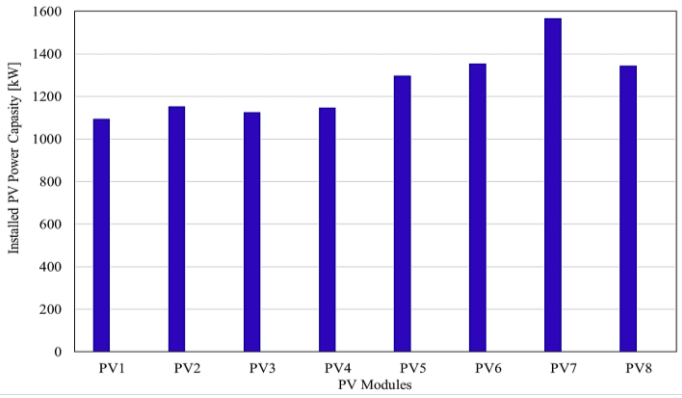

(b)

Figure 4. Comparison of occupation ratios and PV power capacity: (**a**) Comparison of occupation ratios for all PV modules; (**b**) Comparison of installed PV power capacity for a given land area of 10000 m^2

FOREX Publication
Open Access | Rapid and quality publishing
International Journal of Electrical and Electronics Research (IJEER)
Research Article | Volume 12, Issue 3 | Pages 951-956 | e-ISSN: 2347-470X

In this paper, the effectiveness of the given land area utilization is considered. *Figure 4(b)* presents a comparison of installed PV power capacity based on PVsyst software. For a given land area of 10000 m^2, PV7 has the highest installed PV power capacity of 1568 kW, which is 43.32% greater than PV1's lowest installed PV power capacity (1094 kW).

3.3. Net Energy Production

Based on PVsyst's simulation results, *figure 5* compares the net energy production of all PV modules (PV1 through PV8). PV7, with its high installed PV power capacity and low temperature coefficient of P_m, can achieve the highest monthly output energy and a total of 2269029 kWh/year.

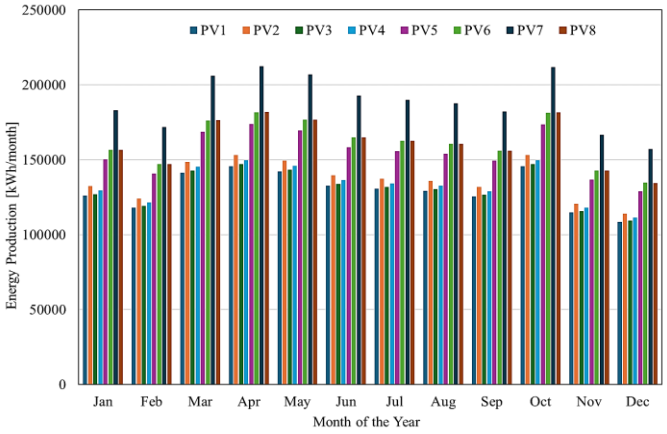

Figure 5. Comparison of monthly net energy production of all PV modules

3.4. Performance Ratio

The percentage of PR shows the partial energy production of solar farms ejected into the grid after energy loss deduction, and generally, the high quality of solar farm performance should have a PR above 80% [28]. Figure 6 shows the monthly PR for all PV modules via PVsyst software. PV7 has the highest monthly PR, accounting for 83.4% of the yearly PR. It is evident that PV7 has a higher ability to transfer net energy production to grid utilization compared to the other PV modules.

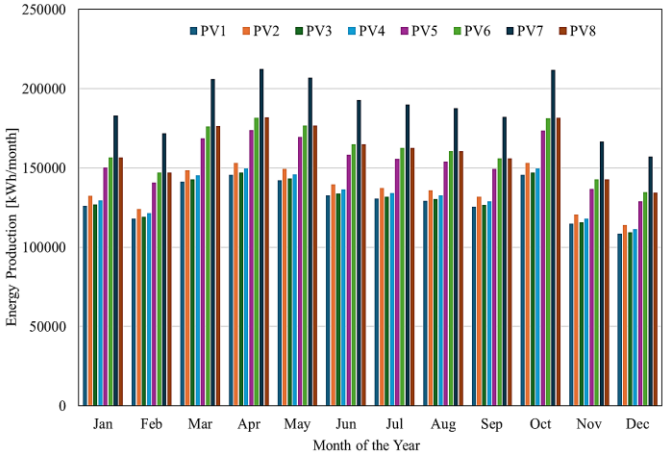

Figure 6. Comparison of monthly performance ratios of all selected PV modules

3.5. Financial Analysis

In the case of financial analysis, only the cost of PV modules, grid tie inverter, land, and selling energy are considered and depicted in *table 3*. *Figure 7* provides a final analysis of the system's cash flow. PV7 has a payback period of approximately 2 years, which is shorter than that of the other 7 PV modules, which have a payback period exceeding 2 years. And after the third year, PV7 provides the highest benefit compared to the other 7 PV modules because PV7's low cost and high energy generation contribute to its effectiveness.

Table 3. System component cost

PV module cost [$/W]							
PV1	**PV2**	**PV3**	**PV4**	**PV5**	**PV6**	**PV7**	**PV 8**
0.2	0.171	0.139	0.139	0.226	0.144	0.13	0.19
Grid tie inverter cost [$/unit]							
2075							
Land cost [$/$m^2$]							
10							
Selling energy cost [$/kWh]							
0.091							

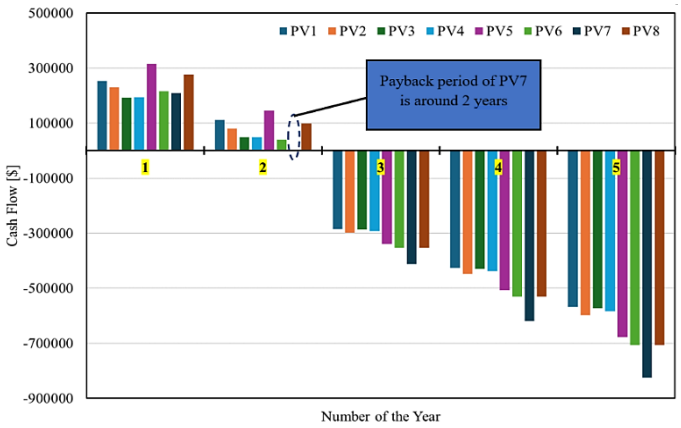

Figure 7. Cash flow of all selected PV modules

4. CONCLUSIONS

In this article, the author only focuses on the performance comparison of eight selected PV modules for solar farm design on given land area 10000 m^2, such as OR, installed PV power capacity, PR, net energy production, and financial analysis. Consequently, the PV modules (PV7), characterized by their high efficiency, low temperature coefficients, and affordable price, result in a significant OR (73.81%), increased installed PV power capacity (1568kW), enhanced energy output (2269029 kWh/year), improved yearly PR (83.4%), and lastly, the shortest payback period (around two years). as a conclusion, three parameters (efficiency, temperature coefficients, and price) of PV module are the key point to improve PV plant performance and cost effectiveness. However, the mounting structure analysis has not been studied yet in this paper. Therefore, the shadow length analysis and M-shape structure

International Journal of
Electrical and Electronics Research (IJEER)
Research Article | Volume 12, Issue 3 | Pages 951-956 | e-ISSN: 2347-470X

will be conducted in this study for future work in order to optimize the PV plant more effectively.

Author Contributions: Conceptualization, S.K.; methodology, S.K.; software, S.K.; validation, S.K., S.N. and C.C.; formal analysis, S.K.; investigation, S.K. and C.C.; resources, S.N.; data curation, H.C.; writing—original draft preparation, S.K.; writing—review and editing, S.K. and C.C; visualization, S.K. and C.C; supervision, D.L.; project administration, D.L.; funding acquisition, D.L and H.C. All authors have read and agreed to the published version of the manuscript.

REFERENCES

[1] United Nations, Department of Economic and Social Affairs, Population Division World Population Prospects 2022: Summary of Results; 2022;

[2] Hao, J.; Wang, L.; Shen, M.; Li, L.; Hu, J. Air Quality Impacts of Power Plant Emissions in Beijing. Environmental Pollution 2007, 147, 401–408, doi:10.1016/j.envpol.2006.06.013.

[3] Open Development Cambodia., Solar Power Plant in Cambodia Available online: https://data.opendevelopmentmekong.net/datastore/dump/6505173f-ed59-412a-a4c0-6ddd27b7b26b (accessed on 7 June 2024).

[4] UNDP Harnessing the Solar Energy Potential in Cambodia; 2019;

[5] Sherwood, L. U.S. Solar Market - Trends 2013; Interstate Renewable Energy Counsil, 2014;

[6] Sherwood, L. U.S. Solar Market - Trends 2008; Interstate Renewable Energy Counsil, 2009;

[7] Future of Solar Photovoltaic: Deployment, Investment, Technology, Grid Integration and Socio-Economic Aspects; International Renewable Energy Agency: Abu Dhabi, 2019; ISBN 978-1-5231-5186-8.

[8] Visal, S.; Shahiduzzaman, Md.; Kuniyoshi, M.; Kaneko, T.; Katsumata, T.; Iwamori, S.; Tomita, K.; Isomura, M. Efficient Planar Perovskite Solar Cells with Entire Low-Temperature Processes via Brookite TiO 2 Nanoparticle Electron Transport Layer. In Proceedings of the 2019 26th International Workshop on Active-Matrix Flatpanel Displays and Devices (AM-FPD); IEEE: Kyoto, Japan, July 2019; pp. 1–4.

[9] Yamamoto, K.; Yoshimi, M.; Tawada, Y.; Okamoto, Y.; Nakajima, A. Thin Film Si Solar Cell Fabricated at Low Temperature. Journal of Non-Crystalline Solids 2000, 266–269, 1082–1087, doi:10.1016/S0022-3093(99)00907-2.

[10] Leng, D.; Polmai, S. Transient Respond Comparison Between Modified Droop Control and Virtual Synchronous Generator in Standalone Microgrid. In Proceedings of the 2019 5th International Conference on Engineering, Applied Sciences and Technology (ICEAST); IEEE: Luang Prabang, Laos, July 2019; pp. 1–4.

[11] Leng, D.; Polmai, S. Virtual Synchronous Generator Based on Hybrid Energy Storage System for PV Power Fluctuation Mitigation. Applied Sciences 2019, 9, 5099, doi:10.3390/app9235099.

[12] Peng, J.; Lu, L.; Yang, H. Review on Life Cycle Assessment of Energy Payback and Greenhouse Gas Emission of Solar Photovoltaic Systems. Renewable and Sustainable Energy Reviews 2013, 19, 255–274, doi:10.1016/j.rser.2012.11.035.

[13] Gopalan, K.; Venkataraman, M. Affordable Housing: Policy and Practice in India. IIMB Management Review 2015, 27, 129–140, doi:10.1016/j.iimb.2015.03.003.

[14] Gong, X.; Kulkarni, M. Design Optimization of a Large-Scale Rooftop Photovoltaic System. Solar Energy 2005, 78, 362–374, doi:10.1016/j.solener.2004.08.008.

[15] Shang, H.; Shen, W. Design and Implementation of a Dual-Axis Solar Tracking System. Energies 2023, 16, 6330, doi:10.3390/en16176330.

[16] Soth, P.; San, S.; Cheng, H.; Tang, H.; Torn, V.; Choeung, C. Voltage Regulation of a Three-Phase PV-Connected Inverter Using LMI-Based Optimization. In Proceedings of the 2023 International Conference on Advanced Mechatronics, Intelligent Manufacture and Industrial Automation (ICAMIMIA); IEEE: Surabaya, Indonesia, November 14 2023; pp. 1–5.

[17] Omar, M.A.; Mahmoud, M.M. Design and Simulation of a PV System Operating in Grid-Connected and Stand-Alone Modes for Areas of Daily Grid Blackouts. International Journal of Photoenergy 2019, 2019, 1–9, doi:10.1155/2019/5216583.

[18] Tamoor, M.; Habib, S.; Bhatti, A.R.; Butt, A.D.; Awan, A.B.; Ahmed, E.M. Designing and Energy Estimation of Photovoltaic Energy Generation System and Prediction of Plant Performance with the Variation of Tilt Angle and Interrow Spacing. Sustainability 2022, 14, 627, doi:10.3390/su14020627.

[19] Odungat, M.M.; Simon, S.P.; Ark Kumar, K.; Sundareswaran, K.; Srinivasarao Nayak, P.; Padhy, N.P. Estimation of System Efficiency and Utilisation Factor of a Mirror Integrated Solar PV System. IET Renewable Power Generation 2020, 14, 1677–1687.

[20] Al Masud, Md.A.; Abedien, M.; Arafi, A.; Abadin, Md.J.; Islam, Md.R.; Haque, Md.S. Performance Optimization of Solar Photovoltaic System Using Parabolic Trough and Fresnel Mirror Solar Concentrator. SSRG-IJEEE 2021, 8, 8–14, doi:10.14445/23488379/IJEEE-V8I6P102.

[21] Kumar, P.; Dubey, R. Efficiency Improvement of Photovoltaic Panels by Design Improvement of Cooling System Using Back Water-Cooling Tubes. International Journal of Engineering Research & Technology (IJERT) 2018, 7, 74–77.

[22] Abbood, A.A.; Salih, M.A.; Mohammed, A.Y. Modeling and Simulation of 1mw Grid Connected Photovoltaic System in Karbala City. International Journal of Energy and Environment 2018, 9, 153–168.

[23] Rehman, S.; Ahmed, M.A.; Mohamed, M.H.; Al-Sulaiman, F.A. Feasibility Study of the Grid Connected 10 MW Installed Capacity PV Power Plants in Saudi Arabia. Renewable and Sustainable Energy Reviews 2017, 80, 319–329, doi:10.1016/j.rser.2017.05.218.

[24] Rachchh, R.; Kumar, M.; Tripathi, B. Solar Photovoltaic System Design Optimization by Shading Analysis to Maximize Energy Generation from Limited Urban Area. Energy Conversion and Management 2016, 115, 244–252, doi:10.1016/j.enconman.2016.02.059.

[25] Balo, F.; Şağbanşua, L. The Selection of the Best Solar Panel for the Photovoltaic System Design by Using AHP. Energy Procedia 2016, 100, 50–53, doi:10.1016/j.egypro.2016.10.151.

[26] Stapleton, G.; Neill, S. Grid-Connected Solar Electric Systems: The Earthscan Expert Handbook for Planning, Design and Installation; Routledge, 2012; ISBN 0-203-58862-2.

[27] Messenger, R.A.; Abtahi, A. Photovoltaic Systems Engineering; CRC press, 2018; ISBN 1-315-21839-9.

[28] Performance Ratio Available online: https://files.sma.de/downloads/Perfratio-TI-en-11.pdf (accessed on 7 June 2024).